The orientational relaxation dynamics were shown to be directly connected with the strength of the two H-bond groups, where the weak H-bonds relax much faster than the strong H-bonds. According to our results, the number of strong H-bonds in the liquid is substantially smaller than expected, which may seem in contradiction with the small heat of melting compared with the heat of sublimation for ice. However, quantum chemical calculations have shown that each bond in the proposed SD configurations is stronger than the average bond in four-fold coordination because of anticooperativity effects (*27*, *28*). Thus, the large number of weakened/broken H-bonds in the liquid leads to only a small change in energy. A recently developed quantum chemical model (*1*, *27*) that proposes the predominance in the liquid phase of two hydrogen–bonded water molecules in ring conformations is consistent with our results. Water is a dynamic liquid where H-bonds are continuously broken and reformed (*29*). The present result that water, on the probed subfemtosecond time scale, consists mainly of structures with two strong H-bonds, one donating and one accepting, nonetheless implies that most molecules are arranged in strongly H-bonded chains or rings embedded in a disordered cluster network connected mainly by weak H-bonds.

References and Notes

1. R. Ludwig, *Angew. Chem. Int. Ed. Engl.* **40**, 1808 (2001).
2. A. K. Soper, *Chem. Phys.* **258**, 121 (2000).
3. A. H. Narten, H. A. Levy, *Science* **165**, 447 (1969).
4. T. Head-Gordon, G. Hura, *Chem. Rev.* **102**, 2651 (2002).
5. P. G. Kusalik, I. M. Svishchev, *Science* **265**, 1219 (1994).
6. A. K. Soper, *J. Chem. Phys.* **101**, 6888 (1994).
7. A. A. Chialvo, P. T. Cummings, *J. Phys. Chem.* **100**, 1309 (1996).
8. F. H. Stillinger, *Science* **209**, 451 (1980).
9. J. Stenger, D. Madsen, P. Hamm, E. T. J. Nibbering, T. Elsaesser, *Phys. Rev. Lett.* **87**, 027401 (2001).
10. J. Stöhr, *NEXAFS Spectroscopy* (Springer-Verlag, Berlin, 1992).
11. U. Bergmann *et al.*, *Phys. Rev. B* **66**, 092107 (2002).
12. Details of the materials and methods, and supporting analysis of the experimental data, are available at *Science* Online.
13. S. Myneni *et al.*, *J. Phys. Condens. Matter* **14**, L213 (2002).
14. M. Cavalleri, H. Ogasawara, L. G. M. Pettersson, A. Nilsson, *Chem. Phys. Lett.* **364**, 363 (2002).
15. D. Nordlund *et al.*, unpublished data.
16. A. Glebov, A. P. Graham, A. Menzel, J. P. Toennies, P. Senet, *J. Chem. Phys.* **112**, 11011 (2000).
17. The ice spectrum (Fig. 1, curve a) has been broadened to the same instrumental resolution as for XRS and normalized to the same area before subtraction.
18. M. Nyberg, M. Odelius, A. Nilsson, L. G. M. Pettersson, *J. Chem. Phys.* **119**, 12577 (2003).
19. A. Luzar, D. Chandler, *Phys. Rev. Lett.* **76**, 928 (1996).
20. K. R. Wilson *et al.*, *J. Phys. Condens. Matter* **14**, L221 (2002).
21. The sharper main edge for hot water (537 eV, Fig. 1, curve e, dashed line) is accounted for by a different balance inside the group of SD species, where more of the H-bond acceptor molecules have distances closer to the AB boundary, i.e., have a larger r_2 and/or θ_2 but still remain in zone A (more Fig. 3A, curve g, and less curve c, e.g.). Accordingly, the intensity decrease above the isosbestic point with temperature can be mainly assigned to the loss of DD configurations with tetrahedral and near tetrahedral environments by 5 to 10% and an increase of SD configurations with H-bond acceptor molecules being closer to the AB boundary.
22. The neutron O-O RDF in (*2*) is very similar to the most recently derived O-O RDF from x-ray diffraction in (*4*).
23. K. Toukan, A. Rahman, *Phys. Rev. B* **31**, 2643 (1985).
24. G. C. Lie, E. Clementi, *Phys. Rev. A.* **33**, 2679 (1986).
25. P. L. Silvestrelli, M. Parrinello, *J. Chem. Phys.* **111**, 3572 (1999).
26. S. Woutersen, U. Emmerichs, H. J. Bakker, *Science* **278**, 658 (1997).
27. F. Weinhold, *J. Chem. Phys.* **109**, 373 (1998).
28. L. Ojamäe, K. Hermansson, *J. Phys. Chem.* **98**, 4271 (1994).
29. C. J. Fecko, J. D. Eaves, J. J. Loparo, A. Tokmakoff, P. L. Geissler, *Science* **301**, 1698 (2003).

30. Supported by the Swedish Foundation for Strategic Research, Swedish Natural Science Research Council, and U.S. National Science Foundation grant CHE-0089215. Generous grants of computer time at the Swedish National Supercomputer Center and the Center for Parallel Computing are gratefully acknowledged. Portions of this research were carried out at the Stanford Synchrotron Radiation Laboratory, a national user facility operated by Stanford University on behalf of the U.S. Department of Energy, Office of Basic Energy Sciences. Use of the Advanced Photon Source (APS) was supported by the U.S. Department of Energy, Basic Energy Sciences, Office of Science, under contract No. W-31-109-ENG-38. Biophysics Collaborative Access Team (BioCAT) is a National Institutes of Health–supported Research Center RR-08630. The Advanced Light Source (ALS) is supported by the Director, Office of Science, Office of Basic Energy Sciences, Materials Sciences Division, of the U.S. Department of Energy under Contract No. DE-AC03-76SF00098 at Lawrence Berkeley National Laboratory. Assistance by the APS, ALS, and the Swedish national laboratory MAX-lab staff is gratefully acknowledged. We thank J. B. Hastings for his valuable comments and discussions and S. P. Cramer for making the XRS spectrometer available.

Supporting Online Material
www.sciencemag.org/cgi/content/full/1096205/DC1
Materials and Methods
SOM Text
Figs. S1 to S11
Tables S1 and S2
References and Notes

29 January 2004; accepted 25 March 2004
Published online 1 April 2004;
10.1126/science.1096205
Include this information when citing this paper.

Asphalt Volcanism and Chemosynthetic Life in the Campeche Knolls, Gulf of Mexico

I. R. MacDonald,[1]* G. Bohrmann,[2] E. Escobar,[3] F. Abegg,[2] P. Blanchon,[4] V. Blinova,[2] W. Brückmann,[5] M. Drews,[5] A. Eisenhauer,[5] X. Han,[6] K. Heeschen,[2] F. Meier,[2] C. Mortera,[7] T. Naehr,[1] B. Orcutt,[8] B. Bernard,[9] J. Brooks,[9] M. de Faragó[10]

In the Campeche Knolls, in the southern Gulf of Mexico, lava-like flows of solidified asphalt cover more than 1 square kilometer of the rim of a dissected salt dome at a depth of 3000 meters below sea level. Chemosynthetic tubeworms and bivalves colonize the sea floor near the asphalt, which chilled and contracted after discharge. The site also includes oil seeps, gas hydrate deposits, locally anoxic sediments, and slabs of authigenic carbonate. Asphalt volcanism creates a habitat for chemosynthetic life that may be widespread at great depth in the Gulf of Mexico.

Salt tectonism in the Gulf of Mexico hydrocarbon province controls the development of reservoirs and faults that allow oil and gas to escape at the sea floor (*1*). More than 30 years ago, investigators studying the Gulf's abyssal petroleum system (*2*) photographed an asphalt deposit (*3*) among salt domes in the southern Gulf of Mexico. During exploration of the Campeche Knolls, about 200 km south of the photographed site (Fig. 1, A and C), we have now found numerous, deeply dissected salt domes with extensive slumps and mass wasting at depths of 3000 m or greater. Massive, lava-like flow fields of solidified asphalt, evidently discharged at temperatures higher than the ambient bottom water (4°C), have been colonized by an abundant chemosynthetic fauna.

The Campeche Knolls are salt diapirs rising from an evaporite deposit that underlies the entire slope region (*4*) and hosts the Campeche offshore oil fields (*5*). Numerous reservoir and seal facies have also been at-

[1]Physical and Life Sciences Department, Texas A & M University–Corpus Christi, 6300 Ocean Drive, Corpus Christi, TX 78412, USA. [2]Fachbereich 5 Geowissenschaften, University Bremen, D-28334 Bremen, Germany. [3]Universidad Nacional Autonoma de Mexico, Instituto de Ciencias del Mar y Limnologìa, Apartado Postal 70-305, Mexico 045510, D.F. Mexico. [4]Instituto de Ciencias del Mar y Limnologìa, Apartado Postal 1152, Cancún, D.F. Mexico. [5]IFM-GEOMAR, Leibniz-Institut für Meereswissenschaften, D-24148 Kiel, Germany. [6]Second Institute of Oceanography, State Oceanic Administration, Zhejiang 310012, China. [7]Universidad Nacional Autonoma de Mexico, Instituto de Geofisica, Mexico, 04510, D.F. Mexico. [8]University of Georgia, 220 Marine Sciences Building, Athens, GA 30602, USA. [9]TDI-Brooks International, Inc. 1902 Pinion, College Station, TX 77845, USA. [10]Aurensis, SA, San Francisco de Sales 38, 28003, Madrid, Spain.

*To whom correspondence should be addressed. E-mail: imacdonald@falcon.tamucc.edu

tributed to breccia associated with the Chicxulub impact, which occurred ~200 km to the east (*6*). Guided by data from satellite imagery (*7*) that showed evidence for persistent oil seeps in this region (*8*), we mapped the bathymetry of a 57-by-87-km area with the German ship *RV Sonne* (*9*).

Resulting swath data show that the northern Campeche Knolls are distinct, elongated hills that average 5 by 10 km in size, with reliefs of 450 to 800 m and slopes of 10 to 20% (Fig. 1A). The crests and flanks on 9 of the 22 knolls mapped contain linear and crescent-shaped faults and slump scarps. In many cases, the slumps are associated with downslope sediment lobes that extend as far as 4 km out over the adjacent sea floor. The locations of persistent oil seeps detected by satellite correspond to the dissected salt structures, which indicate that considerable sea-floor instability is associated with hydrocarbon discharge.

Visual surveys of one dissected knoll (21°54′N by 93°26′W), which we named Chapopote (*10*), revealed extensive surface deposits of solidified asphalt, emanating from points along the southern rim of a broad, craterlike graben near the crest of the structure (Fig. 1B). One subcircular flow measured at least 15 m across and comprised numerous concentric lobes stacked higher toward the center; the entire flow was fractured by ramifying radial joints (Fig. 2, A and B). Other flows were linear, bifurcated in places, up to 20 m wide or greater, and extended far down the slope. The morphologies of these deposits were often blocky (Fig. 2B) or ropy (Fig. 2C), similar to a'a or pa'hoehoe basaltic lava flows. The video and navigation data indicate that asphalt flows cover almost 1 km^2 of the upper structure.

The biological community at Chapopote was extensive and diverse. Concave joints in the ropy asphalt were coated with white microbial films (Fig. 2C). Vestimentiferan tubeworms (cf. *Lamellibrachia* sp.) were common, but were always observed in close proximity to asphalt flows, which they colonized by extending the posterior ends of their tubes into sediments beneath the flow edges (Fig. 2A) or into fissures (Fig. 2D). Some tubeworm aggregations were completely embedded in solidified tar, indicating that they were later overcome by flows (Fig. 2E). Large bivalve shells, including the chemosynthetic family Vesicomyidae (cf. *Calyptogena* sp.), were widespread on the sea floor surrounding the asphalt flows and among asphalt pillows and cobbles (Fig. 2F). Shells and living specimens of chemosynthetic mussels (cf. *Bathymodiolus* sp. and *Solemya* sp.) were recovered by grab sample along with highly oiled sediments. Heterotrophic fauna included galatheid crabs (*Munidopsis* sp.) and shrimp resembling *Alvinocaris* sp., as well as nonendemic deep-sea fish and invertebrates (*Benthodytes* sp., *Psychropotes* sp., and *Pterasterias* sp.). Crinoids and soft corals were attached to asphalt pillows found farthest downslope from the rim.

A video-guided grab recovered ~75 kg of asphalt, tubeworm tubes, and additional associated sediments from the crest of the knoll (Fig. 1B). There was scant hydrocarbon gas and no oil in these sediments (*11*) (Table 1). The asphalt pieces included small fragments and large, irregular blocks weighing more than 10 kg. This material, which was brittle and had no residual stickiness, shows columnar jointing and chilled margins that indicate molten flow followed by rapid cooling (fig. S1). A medical computerized tomography scan of one of the large blocks revealed a relatively low-density mass with an outer, "weathering" rind, an interior with regular folding, and numerous occluded pebbles, the density of which resembled carbonate (fig. S2). Sediments surrounding the asphalt were composed of a thin layer of brown organic material overlying clayey, nannofossil ooze. No H_2S was detected (the detection limit was 2 μM), and the presence of NO_3^- in a gradient from 14 to 4 μM over sediment depths from ~1 to 10 cm below the interface indicated that the surface sediments were oxidized.

A second grab targeted one of the few bacterial mats observed at Chapopote. About 20% of this sample volume consisted of viscous, liquid petroleum dispersed in veins and pockets; asphalt was entirely absent. A surface crust comprised slabs of authigenic carbonate with layers of oil pooled beneath. Sediments were entirely anoxic with H_2S concentrations of 8 to 13 mM. Gas hydrate

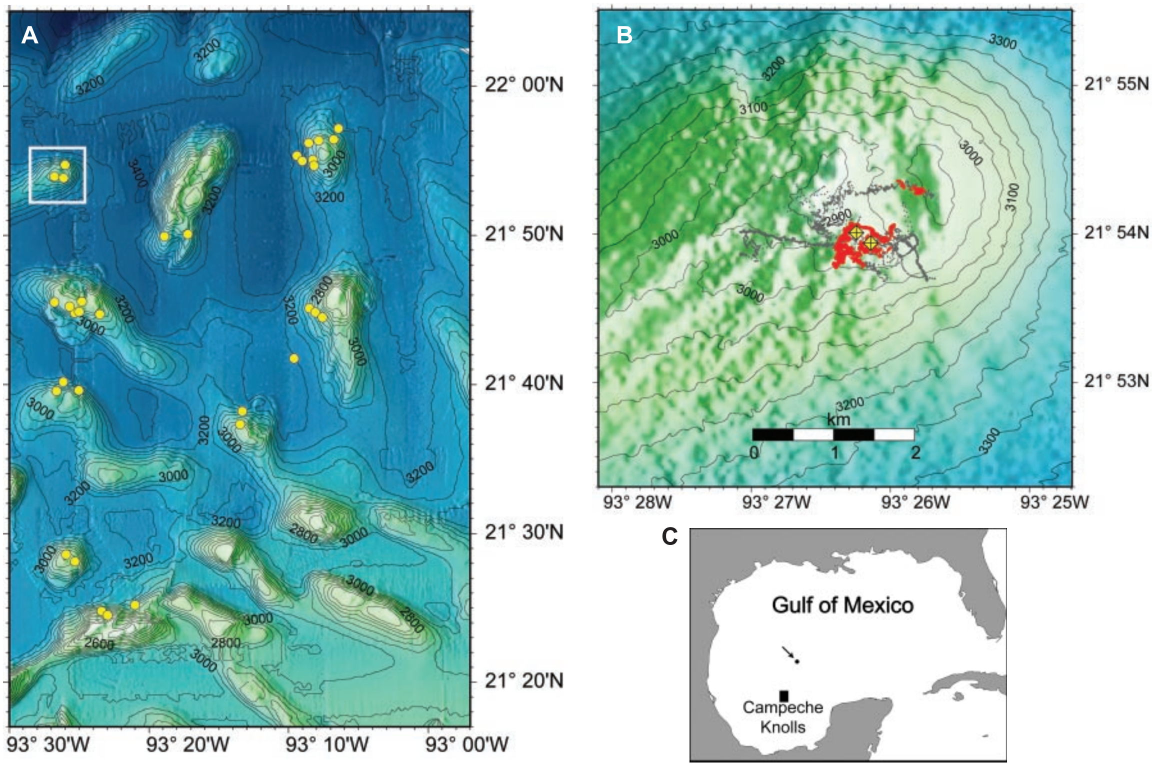

Fig. 1. (**A** and **B**) Maps of (A) the swath-mapped region of the Campeche Knolls and (B) the Chapopote site were compiled onboard the *RV Sonne*. Contour lines are in meters below sea level. Yellow dots mark locations where floating oil was seen in satellite images throughout the knolls. Gray dots mark bottom navigation fixes during the photo-sled survey of Chapopote. Red dots show locations of asphalt pieces or asphalt flows. Yellow diamonds are grab-sample locations. (**C**) The regional setting of the swath map (rectangle) and the location of a 1971 photograph (*3*) of an asphalt pillow (arrow).

formed thin layers in the surface sediments, and numerous pieces floated in the surface water as the grab was recovered on board the ship. A negative chloride anomaly (482 mM) in the upper 4 cm was consistent with gas hydrate layers. An alkalinity profile showed extremely high values from 29 to 35 mM, which indicate the oxidation of hydrocarbons by reduction of seawater sulfate.

Molecular and isotopic compositions of the gas hydrate and sediment headspace from the second grab sample indicate moderately mature, thermogenic gas (Table 1). Aliphatic and aromatic biological markers indicate an Upper Jurassic–sourced, carbonate-rich oil of at least moderate maturity, which is typical of deep-water hydrocarbon seeps in the Gulf of Mexico (*12*). Oily sediment extracts and asphalt pieces were composed of a degraded, unresolved complex mixture of hydrocarbons with a peak at n-C_{30} and a few resolved C_{29} to C_{32} hopanes. Concentration of carbon dioxide in the oily sediment is high compared to values from deep-water sediments of the Gulf of Mexico (*13*). The high concentration of carbon dioxide with a heavy carbon isotopic composition may represent carbon dioxide migrating from a deep source with the hydrocarbons or the dissolution of sediment carbonates under acid conditions.

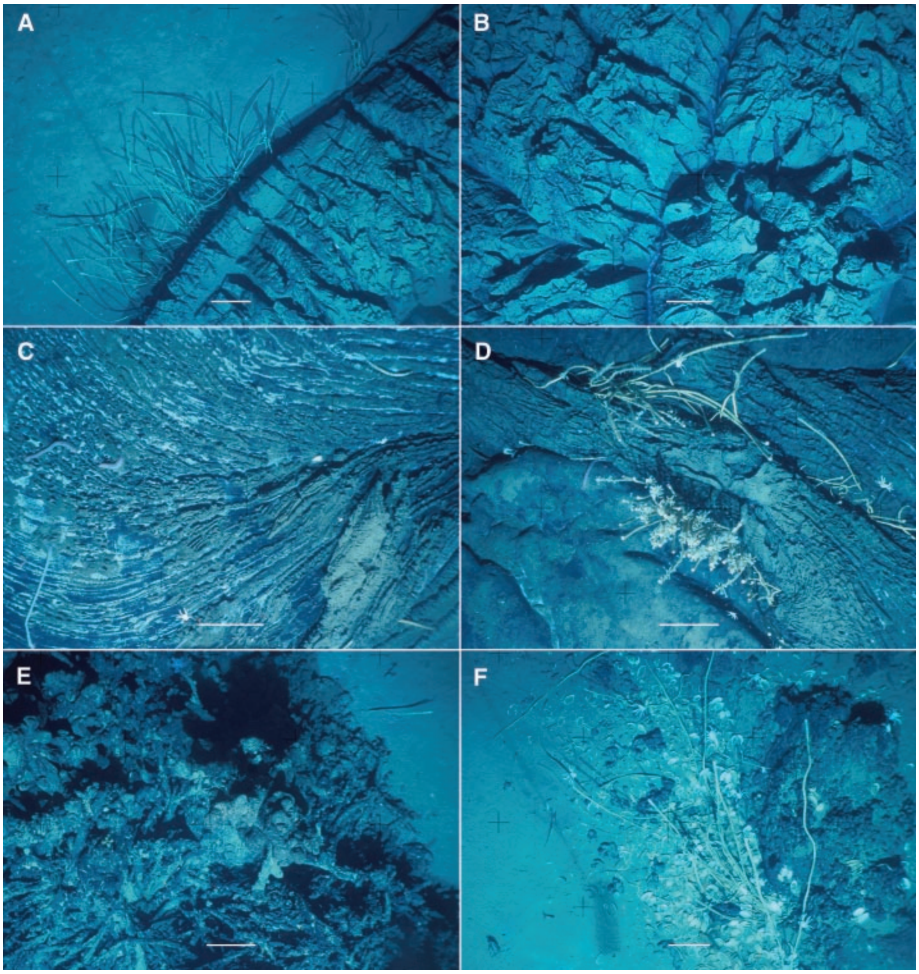

Fig. 2. Photographs of asphalt flows and associated organisms at Chapopote were taken with a remote photo-sled. Scale bars are ~20 cm as determined by parallel lasers projected on sloping sea floor. (**A**) Asphalt flows typically had shrink fractures normal to the flow direction. (**B**) Blocky a'a-like morphology was found in the center of flows measuring ~20 m across. (**C**) Pa'hoehoe-like folds in the freshest materials were lined with white mats or films. (**D**) Clusters of living tubeworms were observed growing through fissures in asphalt. (**E**) Some vestimentiferan clusters appeared to have become embedded in tar. (**F**) At the edges of the flow field, small clusters of vestimentiferans grew under eroded asphalt deposits with living *Calyptogena*, bivalve shells, and galatheid crabs.

Table 1. Hydrocarbon gas composition of sediment and gas hydrate collected in video-guided grabs from Chapopote. Gas hydrate concentrations (Conc.) are reported as parts per million by volume (ppmv) of hydrate gas. Sediment gas concentrations are reported as ppmv of interstitial water. Stable carbon isotopes ($\delta^{13}C$) are reported as parts per thousand relative to Pee Dee Belemnite standard.

Sample	CO_2		Methane		Ethane		Propane		*i*-Butane		*n*-Butane
	Conc.	$\delta^{13}C$	Conc.	$\delta^{13}C$	Conc.	$\delta^{13}C$	Conc.	$\delta^{13}C$	Conc.	$\delta^{13}C$	Conc.
Gas hydrate	3,000	−19.9	962,000	−50.1	29,000	−33.2	33,000	−27.1	8,000	−27.6	1,700
Oily sediment	22,200	−7.5	47,400	−55.1	4,830	−34.1	9,217	−29	6,660	−39.9	295
Asphalt sediment	1,330		17.4		1.5		0.8		0.04		0.2

The size, extent, and morphology of the asphalt flows observed at Chapopote entirely distinguish asphalt volcanism from irregular mats and pools of viscous tar described from coastal (*14*) and continental slope (*15*) oil seeps. Furthermore, the chemosynthetic biota at Campeche Knolls exploit a variety of biogeochemical niches within the site, including an unexplained association with asphalt. Localized seepage of oil and gas produces gas hydrate, oil-saturated sediments, and oil traces that float to the ocean surface. High concentrations of H_2S within the upper sediment column at these localities result from the anaerobic oxidation of hydrocarbon (*16*, *17*), generating authigenic carbonates and a more typical substratum for *Lamellibrachia* (*18*). In contrast, sediments associated with asphalt flows may remain little altered by anaerobic oxidation of hydrocarbons; additional biogeochemical processes must occur within or beneath the asphalt flows to support the prevalent tubeworm aggregations.

The collective data indicate that Chapopote has been subjected to repeated, extensive eruptions of molten asphalt under conditions that are probably incompatible with gas hydrate stability (*19*). The mechanical energy of these eruptions coupled with the violent destabilization of gas hydrate deposits contribute to the faulting, slope failures, and mass wasting mapped at Chapopote and other salt domes in the Campeche Knolls. Additional sampling and measurement will be required to clarify the characteristics of asphalt discharge and the biogeochemical processes that allow chemosynthetic organisms to thrive in association with asphalt deposits. Pequegnat's 1971 photograph (*3*) of an asphalt pillow shows lava-like morphology as well as a galatheid crab, a crinoid, and, although it was not noted by the author, a solitary vestimentiferan (fig. S3). Asphalt volcanism and associated deep-sea life may therefore be a widespread process in the Gulf of Mexico abyss. Satellite surveillance could be an effective tool for finding more of these features.

References and Notes

1. D. Macgregor, *Mar. Petrol. Geol.* **10**, 606 (1993).
2. A. H. Bouma, R. Rezak, L. M. Jeffrey, *Trans. Gulf Coast Assoc. Geol. Soc.* **19**, 115 (1969).
3. W. E. Pequegnat, L. M. Jeffrey, *Contrib. Mar. Sci.* **22**, 63 (1978).

4. W. R. Bryant, J. Lugo, C. Cordova, A. Salvador, in *The Gulf of Mexico Basin*, A. Salvador, Ed. (Geological Society of America, Boulder, CO, 1991), vol. J., pp. 13–30.
5. T. E. Ewing, in *The Gulf of Mexico Basin*, A. Salvador, Ed. (Geological Society of America, Boulder, CO, 1991), vol. J., pp. 31–52.
6. J. M. Grajales-Nishimura *et al.*, *Geology* **28**, 307 (2000).
7. I. R. MacDonald *et al.*, *J. Geophys. Res.* **98 C9**, 16351 (1993).
8. Synthetic aperture radar images collected by RADARSAT and analyzed by NPA Group showed regular patterns of reduced backscatter produced by the dampening of capillary wavelets in elongate patches of floating oil. Repeated occurrences of these targets in the same locality are taken as robust evidence for oil discharge from the corresponding sea bed.
9. Mapping was performed with a Simrad EM120 swath-mapping echosounder.
10. "Chapopote," derived from the Aztec language Nahuatl, means "tar" in Mexican Spanish.
11. Samples of sediment (~75 cc), including oil or asphalt components, were placed with 200 ml of clean seawater into 500-ml containers that were promptly sealed and stored frozen. Small pieces (~5 cc) of gas hydrate received similar treatment, except that the headspace of the containers was purged with nitrogen before they were sealed. Carbon content was determined by gas chromatography of headspace gases and solvent extracts of oil and asphalt.
12. G. A. Cole *et al.*, *World Oil* **2001** (October), p. 69 (2001).
13. TDI-Brooks International, "2000 Central Gulf of Mexico Surface Geochemical Exploration," *Tech. Report No. 01-698* (TDI-Brooks, College Station, TX, 2001).
14. J. S. Hornafius, D. Quigley, B. P. Luyendyk, *J. Geophys. Res.* **104 C9**, 20 (1999).
15. I. R. MacDonald, W. W. Sager, M. B. Peccini, *Mar. Geol.* **198**, 133 (2003).
16. P. Aharon, B. S. Fu, *Geochim. Cosmochim. Acta* **64**, 233 (2000).
17. S. B. Joye *et al.*, *Chem. Geol.*, in press; published online 12 March 2004.
18. D. C. Bergquist *et al.*, *Mar. Ecol. Pubbl. Stn. Zool. Napoli I* **24**, 31 (2003).
19. E. D. Sloan Jr., *Clathrate Hydrates of Natural Gases* (Marcel Dekker, New York, ed. 2, 1998), pp. 705.
20. This is publication GEOTECH-62 of the program GEOTECHNOLOGIEN and publication no. 130 of the Deutsche Forschungsgemeinschaft-Research Center "Ocean Margins" of the University of Bremen. *RV Sonne* cruise SO174 was supported by the German Federal Ministry of Education and Research (Bundesministerium für Bildung und Forschung; grant nos. 03G0174A and 03G0566A). Support for the joint U.S.-Mexican-German participation was provided by the NOAA Office of Ocean Exploration, NSF grant no. OCE-0085548, Universidad Nacional Autonoma de Mexico, and the Harte Research Institute. Also supported by the U.S. Department of Energy, National Energy Technology Laboratory (I.R.M.).

Supporting Online Material
www.sciencemag.org/cgi/content/full/304/5673/999/DC1
Materials and Methods
Figs. S1 to S3
References and Notes

24 February 2003; accepted 31 March 2004

Hydrocarbons in Hydrothermal Vent Fluids: The Role of Chromium-Bearing Catalysts

Dionysis I. Foustoukos* and William E. Seyfried Jr.

Fischer-Tropsch type (FTT) synthesis has long been proposed to account for the existence of hydrocarbons in hydrothermal fluids. We show that iron- and chromium-bearing minerals catalyze the abiotic formation of hydrocarbons. In addition to production of methane (CH_{4aq}), we report abiotic generation of ethane (C_2H_{6aq}) and propane (C_3H_{8aq}) by mineral-catalyzed hydrothermal reactions at 390°C and 400 bars. Results suggest that the chromium component in ultramafic rocks could be an important factor for FTT synthesis during water-rock interaction in mid-ocean ridge hydrothermal systems. This in turn could help to support microbial communities now recognized in the subsurface at deep-sea vents.

Vent fluids issuing from ultramafic-hosted hydrothermal systems at mid-ocean ridges not only contain abundant methane but are also enriched in propane, ethane, and many other dissolved hydrocarbons (*1*, *2*). It is likely that the occurrence and distribution of these hydrocarbons is the result of FTT synthesis, where oxidized forms of dissolved carbon are reduced to hydrocarbons by reaction with H_{2aq}. In general, this process can be described schematically as follows:

$$CO_{2aq} + [2 + (m/2n)]H_{2aq} \rightarrow (1/n)C_nH_m + 2H_2O \quad (1)$$

The formation and distribution of alkanes produced in hydrothermal experiments at elevated pressure and temperature suggest that the reactions are catalyzed by minerals (*3*). As such, the chemical and physical properties of the catalyst play a key role in hydrocarbon yield. For example, formation of relatively small amounts of methane was reported in experiments involving reaction of CO_2-bearing aqueous fluid with different minerals (hematite, magnetite, olivine, serpentine, and Ni-Fe alloy) (*4*, *5*). The Ni-Fe alloy (awaruite), in particular, appears to be an excellent catalyst for CO_{2aq} conversion to CH_{4aq} (*6*). Although abiotic methane was inorganically generated during these experiments, no other alkanes were produced. The relative lack of hydrocarbons other than methane, however, brings into question an origin by FTT synthesis of the complex hydrocarbons in vent fluids issuing from ultramafic-hosted hydrothermal systems (*7*). McCollom and Seewald (*5*) speculated that it is only in the presence of a discrete gas phase that abiotic synthesis of the more complex hydrocarbon species may be at all possible. Here, we report results of a hydrothermal experiment indicating that Fe-Cr oxide (e.g., chromite) is a catalyst for FTT synthesis of longer chain hydrocarbons. The chromium content of fresh oceanic ultramafic rocks is nearly 3000 ppm (*8–10*) and is preferentially concentrated in orthopyroxene (*11*, *12*), a particularly reactive mineral in ultramafic rocks (*3*, *13*). Orthopyroxene alteration can be expected to provide Cr for chromite, a common accessory mineral, especially in enstatite-rich peridotite or bastite.

Our experiments were performed at 390°C and 400 bars, conditions that approximate those inferred for ultramafic-hosted hydrothermal alteration at Rainbow (36°N) and Logatchev (14°N) on the Mid-Atlantic Ridge (*1*, *2*, *7*). In addition to abundant hydrocarbons, vent fluids from these hydrothermal systems have substantial amounts of dissolved H_{2aq} (*2*). Reducing conditions undoubtedly result from the hydrolysis of olivine, or more likely orthopyroxene, giving rise to the formation of magnetite together with talc and/or serpentine (*3*, *13*).

Experiments were conducted in a flexible gold-cell hydrothermal apparatus (*14*), which allows fluid sampling at experimental conditions while also permitting introduction of fluid reactants (*15*). An added advantage of the gold-titanium reaction cell is its inherent lack of catalytic activity. Therefore, high dissolved concentrations of CO_2 and H_2 can coexist for long intervals at temperatures and pressures as high as 400°C and 500 bars without generation of appreciable amounts of reduced carbon species (*16*). Thus, in the absence of appropriate mineral catalysts, generation of reduced carbon species is inhibited.

To trace carbon sources and sinks during the experiment, we added ^{13}C-enriched $NaHCO_3$ (~99% ^{13}C) to the fluid. The starting fluid also contained NaCl (0.56 mol/kg) to approximate the bulk chemistry of axial vent fluids. Moreover, to facilitate chromite formation under highly reducing conditions (*17*), FeO was combined with Cr_2O_3 and the ^{13}C-bearing aqueous fluid (*18*). The existence of FeO in amounts greater than needed to form stoichiometric chromite permitted the formation of mag-

Department of Geology and Geophysics, University of Minnesota, Minneapolis, MN 55455, USA.

*To whom correspondence should be addressed. E-mail: fous0009@umn.edu